arXiv:1703.04659v1 [cond-mat.str-el] 14 Mar 2017

The mother of all states of the kagome quantum antiferromagnet

Hitesh J. Changlani,[1,2] Dmitrii Kochkov,[2] Krishna Kumar,[2] Bryan K. Clark,[2] and Eduardo Fradkin[2]

[1]*Department of Physics and Astronomy, Johns Hopkins University, Baltimore, Maryland 21218, USA*

[2]*Department of Physics and Institute for Condensed Matter Theory, University of Illinois at Urbana-Champaign, 1110 West Green St, Urbana IL 61801, USA*

(Dated: March 16, 2017)

One of the challenges in theoretical condensed matter physics is the physics of strongly correlated systems in regimes in which all interactions are nearly equally strong. This is particularly the case in quantum spin systems on geometrically frustrated lattices where, the inability to simultaneously satisfy competing exchange interactions, often results in the selection of magnetically ordered or exotic disordered spin liquid ground states. We report the existence of a *quantum* macroscopically degenerate ground state manifold in a simple model, the nearest neighbor antiferromagnetic XXZ model on the kagome lattice, for the ratio of Ising to antiferromagnetic transverse coupling $J_z = -1/2$. We explore the panoply of phases that emerge from this exactly solvable point and discuss its wider impact on the phase diagram of the kagome lattice antiferromagnet.

I. INTRODUCTION

The history of quantum frustrated magnetism began in 1973 with the suggestion by Phil Anderson that the ground state of the nearest-neighbor (n.n) Heisenberg model on the triangular lattice was a quantum spin liquid [1]. While we now know that this particular model does not support a spin-liquid, both experimental and theoretical evidence has been building for quantum spin-liquids in various lattices built of triangular motifs. Materials such as Herbertsmithite (a kagome lattice of Cu^{2+} ions) [2] and $Na_4Ir_3O_8$ (a hyperkagome lattice of Ir^{4+} ions) [3] fail to order down to low temperatures suggesting a possible spin liquid ground state. Theoretically, evidence exists for a panoply of spin-liquids and ordered phases on the kagome lattice with varied Hamiltonians [4–13].

Triangular motifs have been considered to be promising places to look for spin-liquids because,

in the Ising limit, geometric frustration prevents the simultaneous minimization of the energy on all three bonds of any triangle. Triangular motifs occur in various finite and extended lattices including the sawtooth, triangular, Shastry-Sutherland [14], kagome, hyperkagome and icosidodecahedron lattices. For some lattices and Hamiltonians, this degeneracy resolves to an ordered state, but others have topological ground states such as spin-liquids. A particular notable case of the latter is in the n.n. spin 1/2 Heisenberg model on the Kagome lattice. Strong numerical evidence exists for a spin-liquid here although there is significant controversy about its qualitative nature [4–7, 9, 11] with suggestions including possible Z_2 or Dirac spin liquid.

II. RESULTS

We report the existence of a new macroscopic *quantum* degenerate point on kagome and hyperkagome lattices in the spin-1/2 XXZ Hamiltonian, [15–20],

$$H_{XXZ}[J_z] = \sum_{\langle i,j \rangle} S_i^x S_j^x + S_i^y S_j^y + J_z \sum_{\langle i,j \rangle} S_i^z S_j^z \tag{1}$$

at $H_{\mathrm{XXZ}}[-1/2]$ (notated as H_{XXZ0} [21]); here S_i are the usual spin-1/2 operators on site i, $\langle i,j \rangle$ refer to nearest neighbor pairs and J_z is the Ising coupling. This degeneracy exists in all non-trivial S_z sectors and all finite system sizes. For kagome, we explicitly demonstrate this in Fig. 1 where we perform an exact diagonalization (ED) on $N = 30$ site kagome clusters in different S_z sectors. As we approach $J_z = -1/2$ many eigenstates collapse to the same ground state eigenvalue.

We solve analytically for much of the exponential manifold. These analytical solutions apply to any lattice of triangular motifs with the Hamiltonian of the form,

$$\sum_{\Delta} H_{XXZ0}(\Delta) \tag{2}$$

where $H_{XXZ0}(\Delta)$ is the $XXZ0$ Hamiltonian on a triangle Δ, as long as the vertices can be colored by three colors with no two connected vertices being assigned the same color. Among the many lattices that fall into this classification, the prominent ones are the kagome, hyperkagome, triangular, Shastry-Sutherland (at $J_2/J_1 = 2$), saw-tooth, zig-zag ladder, and icosidodecahedron lattices, some of which are illustrated, with prototypical three-colorings, in Fig. 2. On the zig-zag ladder, our result overlaps at a special choice of parameters with a different analytically solvable Hamiltonian previously reported by Ref. [22]. While our ground states are exact analytic solutions on any such lattice, only on the kagome and hyper-kagome is their degeneracy macroscopic.

Finally, we consider how the $XXZ0$ point on the kagome lattice is embedded in the wider kagome phase diagram showing its relation to the previously discovered spin liquid at the Heisenberg point [5] as well as nearby $q = 0$ and $\sqrt{3} \times \sqrt{3}$ phases; our results from ED suggest that there are not one but two different spin liquids which transition at the Heisenberg point.

A. Exact Ground States

Any Hamiltonian of the form of Eq. (2) has ground states of the form

$$|C\rangle \equiv P_{S_z}\Big(\prod_{\text{valid}} \otimes |\gamma_s\rangle\Big) \tag{3}$$

where $\{|\gamma_s\rangle = |a\rangle, |b\rangle \text{ or } |c\rangle\}$, labeled "colors" on site s, defined as,

$$|a\rangle \equiv \frac{1}{\sqrt{2}}\Big(|\uparrow\rangle + |\downarrow\rangle\Big) \tag{4a}$$

$$|b\rangle \equiv \frac{1}{\sqrt{2}}\Big(|\uparrow\rangle + \omega|\downarrow\rangle\Big) \tag{4b}$$

$$|c\rangle \equiv \frac{1}{\sqrt{2}}\Big(|\uparrow\rangle + \omega^2|\downarrow\rangle\Big) \tag{4c}$$

where $\omega = \exp(i2\pi/3)$. Taking the quantization axis to be the z-axis, the colors correspond to spin directions in the XY plane that are at 120 degrees relative to one another. "Valid" colorings are those which satisfy the three-coloring condition i.e. no edge contains two identical colors. P_{S_z} projects into a particular total S_z sector.

To see why this is so for $J_z = -1/2$, note that for a single triangle, six states; the ferromagnetic state $|\uparrow\uparrow\uparrow\rangle$ and the chiral states $|\uparrow\downarrow\downarrow\rangle + \omega|\downarrow\uparrow\downarrow\rangle + \omega^2|\downarrow\downarrow\uparrow\rangle$ and $|\uparrow\downarrow\downarrow\rangle + \omega^2|\downarrow\uparrow\downarrow\rangle + \omega|\downarrow\downarrow\uparrow\rangle$ and all their Kramers pairs; are exactly degenerate. The Hamiltonian (2) is then recast as,

$$H = \sum_{\Delta} H_\Delta = \frac{3}{2}\sum_{\Delta} P_\Delta - \frac{3}{8}N_\Delta \tag{5}$$

where N_Δ is the number of triangles and P_Δ is a projector,

$$P_\Delta \equiv |+\rangle\langle+| + |-\rangle\langle-| \tag{6}$$

on the triangle. $|+\rangle$ and $|-\rangle$ are Kramers pairs of non-chiral one-magnon states on the triangle,

$$|+\rangle \equiv \frac{1}{\sqrt{3}}\Big(|\uparrow\uparrow\downarrow\rangle + |\uparrow\downarrow\uparrow\rangle + |\downarrow\uparrow\uparrow\rangle\Big) \tag{7a}$$

$$|-\rangle \equiv \frac{1}{\sqrt{3}}\Big(|\downarrow\downarrow\uparrow\rangle + |\downarrow\uparrow\downarrow\rangle + |\uparrow\downarrow\downarrow\rangle\Big) \tag{7b}$$

This rewriting can be carried out on any lattice of triangles; if a bond is used by multiple triangles this constrains the coupling constant between these bonds. For example, for the Shastry-Sutherland lattice this rewriting is only possible when $J_2/J_1 = 1/2$ as two triangles overlap the bonds across the square while only one triangle overlaps all other bonds. This is to be contrasted with a lattice like the kagome lattice where each bond belongs to only one up or down triangle.

The $XXZ0$ Hamiltonian is thus the sum of positive definite non-commuting projectors. If it is possible to simultaneously zero out each projector consistently, then such a wavefunction is guaranteed to be a ground state. Hamiltonians with this property are called "frustration-free" and are central to the construction of ground states of the Majumdar-Ghosh [23] (generalized by Klein [24]) and Affleck-Kennedy-Lieb-Tasaki [25] Hamiltonians. (There are other classes of exactly solvable models, often with topological ground states [26–28], that involve a sum of commuting projectors.) In our case, zeroing out the projector would require that only components exactly orthogonal to states $|+\rangle$ and $|-\rangle$ enter the full many body wavefunction. This is indeed achieved by the product state $|\psi\rangle \equiv \prod_{\text{valid}} \otimes |\gamma_s\rangle$; one can explicitly check this by calculating $a \otimes b \otimes c$ which has no component in $|+\rangle$ or $|-\rangle$. We refer to these as "three coloring states" and note that they have been studied classically or semi-classically [21, 29–34] on the kagome and on honeycomb lattices in a quantum model [35].

The product state $|\psi\rangle$ does not conserve total S_z but the Hamiltonian *does conserve* it. Therefore, not only is every unprojected three-coloring a ground state, but we can generate many more ground states by projecting every such three-coloring to each S_z sector. We thus have eigensolutions (one for each coloring and projection), of the form Eq. (3). This means that for any lattice there is at least a degeneracy proportional to system size. Note, that the number of 3-colorings that need to be counted are those with a reference site always fixed to a specific color (say a); this is because individual colors can be transformed into one another by gauge transformations which do not alter the many-body wavefunction (up to a phase factor), a subtlety addressed in the Supplemental Information.

B. Macroscopic Degeneracy

While there are only two ways of three-coloring the triangular lattice, there are an exponential number of ways of doing so on the kagome and hyperkagome lattices. This can easily be seen by considering closed loops (such as hexagons on the kagome), which can be two-colored and

independently rotated by one color. Baxter has rigorously calculated the number of three colorings of bonds of the honeycomb lattice (dual to the vertices of the kagome lattice) and shown it to be 1.20872^N for large N [36]. As the unprojected three-colorings are independent this gives an exponential number of ground states.

Additionally, as projected colorings are ground states, it implies macroscopic degeneracy exists in *every* non-trivial S_z sector. The actual number, however, varies from sector to sector because of the loss of linear independence of the unprojected solutions under projection. This is most easily seen if one restricts oneself to the completely spin polarized sector; then all colorings project to exactly the same state. However, for typical S_z of interest, particularly $S_z = 0$, an exponential number of colorings of the kagome and hyperkagome lattices translates to an exponential number of linearly independent solutions as well.

This notion can be made precise by forming the overlap matrix

$$S_{C,C'} \equiv \langle C|C'\rangle = \sum_{s_1+s_2+\ldots s_N=S_z} \langle C|s_1 s_2 \ldots s_N\rangle\langle s_1 s_2 \ldots . s_N|C'\rangle \tag{8}$$

and evaluating its rank $\equiv R(S)$ numerically; our results have been shown in Table I. Even though the Ising sums do not factorize due to the constraint of total $s_1 + s_2 \ldots + s_N = S_z$, a mathematical trick makes the sum tractable by converting the high dimensional summation into a one dimensional one. Further details are discussed in the Supplementary Information.

The case of one down spin in a sea of up spins i.e. $S_z = (N/2) - 1$ is equivalent to a single particle hopping on a kagome lattice with $\pi-$ flux through each triangle (and zero flux through hexagons). This model is known to have a flat-band with a quadratic band touching [37]. As seen in Table I, the projected coloring solutions reproduce the expected degeneracy, $N_h \equiv$the number of unit cells (or hexagons) + 1. Ref. [37] explained this in terms of the $N_h - 1$ linearly independent localized modes (one per hexagon) and the two additional topologically non trivial loops on the torus all of which have the same energy. This shows that, at least in some cases, the coloring space is capable of describing topologically non-trivial modes.

It is interesting to note that the prescription of the exact solution still holds even if we take the value of J on JH_{XXZ0} to be different on different triangles (while the same on all bonds of one triangle). The exact ground states are still the same and there are still a macroscopic number of them on lattices such as kagome and hyperkagome. Two cases where this may be of particular interest is the completely disordered case since this provides an explicit example for a disordered system where a macroscopic degeneracy holds exactly; and in the case where, on the kagome, up

and down triangles carry different strengths as this gives an exactly degenerate ground state as one adiabatically evolves to uncoupled triangles.

C. Additional Ground States

We address the question of whether the three-coloring solutions describe all ground states. On several representative kagome clusters with open boundary conditions (but always with completed triangles) and for various total S_z (see Table I and supplemental information), we never find solutions outside the coloring manifold described above. While we can not rigorously prove that for larger system sizes or different open clusters they do not exist, this suggests the possibility that coloring solutions may indeed be sufficient to describe all degeneracies on these lattices. However, on the torus we do find degenerate solutions not spanned by the coloring solutions. This is because a non-coloring state may become a ground state when projected to definite S_z sector. This is particularly true at low fillings; at half filling, though, we did not find examples where the colorings do not span the manifold of ground states.

D. Connection to the wider Kagome phase diagram

We consider how the $XXZ0$ point is embedded in the larger Kagome phase diagram. We focus on the $S_z = 0$ sector, with the Hamiltonian

$$H[J_z, J_2] = H^{\text{nn}}_{XXZ}[J_z] + J_2 H^{\text{nnn}}_{XXZ}[J_z] \tag{9}$$

where nn and nnn denote the nearest neighbor and next-nearest-neighbor terms respectively. Our objective is to better understand the relation of $XXZ0$ to the previously identified spin-liquid at the Heisenberg point in a range of J_2 [4–7].

To determine the phase diagram in the vicinity of $XXZ0$, we use a combination of analytical arguments and ED on the 36d cluster at a grid of points in the (J_z, J_2) space. As Fig. 3 shows, we find five phases near $XXZ0$: a ferromagnetic phase, a $q = 0$ phase, a $\sqrt{3} \times \sqrt{3}$ phase and (likely) two spin-liquids. We show that all these phases, other than the ferromagnet, are adiabatically connected to the nn and nnn Heisenberg models ($J_z = 1$), suggesting that perturbations from $XXZ0$ are critical to understanding these phases.

At $J_z = -1/2$ and $J_2 > 0$ (notated AF-line) all triangles in the Hamiltonian are of the $XXZ0$ form and remain consistently three-colorable. Three-coloring both nn and nnn triangles constrains

the allowed colorings leaving only two colorings in the well known $q = 0$ pattern. This phase survives for $J_z > -1/2$, at small J_2, and is primarily identified by peaks at the M point in the structure factor $S(\vec{q})$ (see Fig. S 2). On the other hand, it can be analytically shown (see supplement) that the minimum energy state upon perturbing the AF-line to $J_z < -1/2$ is the fully polarized ferromagnetic state.

At $J_z = -1/2$ and $J_2 < 0$, we find evidence for the $\sqrt{3} \times \sqrt{3}$ phase. Here, three-coloring the nnn triangles instead maximizes their energy and we can not solve exactly for the ground state as the corresponding projector is no longer non-negative definite. Instead if, at small $|J_2|$, we consider only those states that consistently three-color the nn triangles, the lowest energy state has all three vertices of each nnn triangle colored with the same color yielding the $\sqrt{3} \times \sqrt{3}$ state. By looking at $S(\vec{q})$ at the K point, from our ED data, we numerically verify this phase and see it survives for J_z near and on both sides of $-1/2$.

By tracing paths through phase space with large values of $S(\vec{q})$ at the K and M points, we find that both the $q = 0$ phase and $\sqrt{3} \times \sqrt{3}$ phases near the $XXZ0$ point extend to the Heisenberg point at non-zero J_2. To locate the boundaries of these phases, we perform sweeps through J_2 at finite J_z and identify dips in the wavefunction fidelity (defined to be the magnitude of the overlap between ground state wavefunctions at adjacent points in parameter space). As Fig 3 shows, for both magnetically ordered phases, the location of these dips form lines emanating from (or close to) the $XXZ0$ point that extrapolate to the Heisenberg point ($J_z = 1$) to values $J_2 \approx 0.16$ for $q = 0$ and $J_2 \approx -0.06$ for $\sqrt{3} \times \sqrt{3}$. These values are within the bounds previously found by a DMRG study [38]. In the intermediate phase(s), we see a decrease in the magnitude of the structure factor peaks consistent with a change in phase to a spin-liquid.

We are unable to directly resolve the question whether the spin liquid phases directly connect to the $XXZ0$ point. Near $XXZ0$ we do not detect fidelity dips and see larger structure factors that extend much closer to the line $J_2 = 0$. This leaves two plausible scenarios: (1) the spin-liquid(s) terminate at $J_z > -1/2$ for all J_2 or (2) the phase boundaries extend to $XXZ0$ but finite size-effects near it become large making it difficult to resolve the transition.

While the current belief is that a single spin liquid phase mediates the phase transition between two magnetically long range ordered phases, we find additional fidelity dips at $J_2 = 0$ and $J_z > -1/2$. This interesting and somewhat unexpected finding strongly suggests the possibility that there is not one but actually two spin liquid phases. To further understand the nature of the fidelity dips, we consider the ground state and excited state in the same quantum number sector as a

function of J_2 at $J_z = 0.1$ (Fig. 4, top right); note that the true first excited-state is in another sector. We see a (formally avoided) "level-crossing" indicated by a shrinking gap between these states around $J_2 = 0$. This crossing causes the fidelity dip and leads to the overlap of the wave-function on both sides of $J_2 = 0$ being small with respect to a reference point on the other side (see Fig. 4, top left). In addition, the structure factors of the two ground states at positive and negative J_z, despite not having large peaks, are qualitatively distinct (see Fig. 4, bottom).

The identity of the ground state of the purely nn kagome antiferromagnetic Heisenberg (KAHF) model has been controversial; recent consensus suggests a spin-liquid but its nature is unclear. Our interpretation would explain some of this controversy as resulting from KAHF being at a critical point in neither phase. We can then speculate about the nature of the two spin liquids above (positive J_2) and below (negative J_2) this point. The qualitative features of the structure factor above and below the transition appear to be consistent with the large N mean field results for Z_2 spin liquids of the $Q_1 = Q_2$ and $Q_1 = -Q_2$ type respectively [33]. The possibility that these are the two spin-liquids is also consistent with a recent IPEPS study [39] which found nearly degenerate variational energies for the $Q_1 = Q_2$ and $Q_1 = -Q_2$ spin liquids. While they interpreted this near degeneracy as evidence for the parent $U(1)$ Dirac spin liquid, in light of our new results, we suggest a more natural interpretation is that the two phases become degenerate at the KAHF critical point.

III. DISCUSSION

In this work, we have (1) shown that H_{XXZ0} is macroscopically degenerate on the kagome and hyperkagome lattices, (2) shown that all projected three-coloring states are exact ground states of H_{XXZ0} on any three-colorable lattice of triangular motifs explaining this macroscopic degeneracy, (3) seen how the $XXZ0$ point is embedded in the $J_2 - J_z$ kagome phase diagram, and (4) given evidence for the possibility that the KAHF is actually a transition between two different spin-liquids.

Our work focuses on lattices of triangular motifs. Such lattices have very different phenomenology at the Heisenberg or XY point but all appear similar in the Ising limit - they are all classically macroscopically degenerate. On the other hand, many of these differences become evident at the $XXZ0$ point suggesting that it controls the physics of the Heisenberg or XY point. For example, our quantum coloring solutions show that the triangular lattice (perturbed slightly in the direction

of Heisenberg) is 120 degree ordered at $XXZ0$; this is also known to be true at the Heisenberg point. It also provides a framework to understand the nearly degenerate manifold which has been reported in the finite icosidodecahedron cluster in the XY regime [40].

On lattices where there is theoretical and/or experimental evidence for spin-liquids, such as the kagome or hyperkagome lattices [3, 41], we find macroscopic degeneracy of the $XXZ0$ ground states. Such a degeneracy is naturally conducive to forming a spin-liquid and is consistent with the large number of low-lying states in KAHF. In fact, on the kagome, we find a spin-liquid phase near $XXZ0$ which extends to the Heisenberg point. Additional nearby (as a function of J_2) co-planar ordered phases are explained by $XXZ0$; the ordered phases (as seen by DMRG) are the nn coloring solutions which have lowest energy at $J_2 \neq 0$; these solutions are adiabatically connected to the Heisenberg point. It is interesting to note that our data suggests a much sharper transition into the ordered phase at $J_2 < 0$ than $J_2 > 0$ as signaled by a sharper jump in the structure factor and fidelity dips which survive to larger J_z; this suggests a possible first-order transition at $J_2 < 0$ and a second order transition at $J_2 > 0$.

While the nature of the KAHF spin-liquid is currently controversial, by considering the larger $J_2 - J_z$ phase diagram we see a clear "level-crossing" at the $J_2 = 0$ line. Such a "level-crossing" strongly suggests the possibility that this is a transition between two different phases and is consistent with the possibility of two different spin-liquids.

The central ideas of the paper are also easily extendable to other frustrated lattices with four (or higher) site motifs, for example by defining four colors on vertices of a square or pyrochlore [42–44] lattice $a \equiv |\uparrow\rangle + |\downarrow\rangle$, $b \equiv |\uparrow\rangle + i|\downarrow\rangle$, $c \equiv |\uparrow\rangle - |\downarrow\rangle$ and $d \equiv |\uparrow\rangle - i|\downarrow\rangle$ (corresponding to spins pointing along +x, +y, -x, and -y respectively) and then writing the projector which annihilates all states that have one a,one b, one c and one d on a square or tetrahedron motif. The Hamiltonian for a single four site motif for this case is,

$$H = \frac{7}{8} + \Big(\sum_{i<j} S_i^+ S_j^- + S_i^- S_j^+ - \frac{1}{2} S_i^z S_j^z \Big) + \sum_{i<j,k<l,\text{diff}} S_i^+ S_j^+ S_k^- S_l^- - 2\, S_1^z S_2^z S_3^z S_4^z \quad (10)$$

where the notation "diff" is used to indicate that all the indices i, j, k, l are distinct. For the square lattice case, this Hamiltonian is in the vicinity of the $J_1 - J_2$ XY model (J_1 and J_2 referring to the nearest and next nearest neighbor/diagonal couplings) with $J_2/J_1 = 1/2$, which has been shown to have a Z_2 spin liquid ground state [45]. The case of the pyrochlore is less well understood, even though other exactly solvable models have been studied [46, 47]. Since the frustration free Hamiltonian in this (and other related) cases is slightly more involved than the simple XXZ

model, it is not further discussed here and will be pursued elsewhere.

Finally, we also note that three coloring states can be used to construct accurate many-body wavefunctions [10, 48–50]. Typically Jastrow factors have been introduced only on top of a single coloring; our present investigation suggests that a linear combination of colorings may provide accurate results in the vicinity of the $XXZ0$ point.

ACKNOWLEDGEMENT

We thank V. Elser, B. Shastry, O. Tchernyshyov, V. Chua, L.D.C Jaubert, S. Sachdev, R. Flint, and O. Benton for discussions and H. Wang for collaboration on related work. HJC, DK and BKC were supported by SciDAC grant DE-FG02-12ER46875 and KK and EF by NSF grant No. DMR 1408713. HJC also acknowledges funding from the IQM (JHU) which is supported by the U.S. Department of Energy, Office of Basic Energy Sciences, Division of Materials Sciences and Engineering under Award DE-FG02-08ER46544. This research is part of the Blue Waters sustained petascale computing project, which is supported by the National Science Foundation (award numbers OCI-0725070 and ACI-1238993) and the State of Illinois.

AUTHOR CONTRIBUTIONS

HJC, EF and BKC conceived the initial ideas and exact solution that led to the development of the project. DK, KK, HJC and BKC wrote the computer codes and DK and HJC performed the calculations and prepared the figures. All authors contributed to the analysis of the data, discussions and writing of the manuscript.

ADDITIONAL INFORMATION

Supplementary Information accompanies this paper.

Competing financial interests: The authors declare no competing financial interests.

METHODS

Numerical techniques

Our primary numerical results come from exact diagonalization calculations based on the Lanczos algorithm. We work in a fully symmetrized basis, exploiting translation and point group symmetries of the 36d cluster shown in Fig. S1 in the Supplemental Information. This reduces the dimensionality of the Hilbert space for a fully symmetric sector to 63044766 basis elements, which is approximately a factor of 144 smaller than the original $S_z = 0$ sector. Although the ground state can belong to any irreducible representation and any momentum sector, by analyzing all of the sectors at points $(J_z, J_2) = \{(-0.3, \pm 0.05), (0, \pm 0.05), (0.1, 0), (0.5, \pm 0.02)\}$ we conclude that it resides in the symmetric sector of $K = (0, 0)$ in the range of interest and focus on investigation of this sector. We base our analysis on the observable quantities such as spin-spin correlation, spin structure factors and ground state fidelity. All these quantities were extracted from the numerical vectors obtained by exact diagonalization. We used the following definitions for fidelity f and spin structure factor $S(\vec{q})$.

$$\begin{aligned} f(x + \frac{h}{2}) &\equiv \langle \psi(x) | \psi(x + h) \rangle \\ S(\vec{q}) &\equiv \frac{1}{N} \sum_{i,j} \langle S_i, S_j \rangle e^{i\vec{q}(\vec{r_i} - \vec{r_j})} \end{aligned} \tag{11}$$

Here h is a step in the parameter space, $\vec{q}$ is a momentum vector on a reciprocal lattice, r_i - real space coordinates of the i^{th} lattice site, and $\langle S_i, S_j \rangle$ is the spin-spin correlation function.

[1] P. Anderson, Materials Research Bulletin **8**, 153 (1973).

[2] J. S. Helton, K. Matan, M. P. Shores, E. A. Nytko, B. M. Bartlett, Y. Yoshida, Y. Takano, A. Suslov, Y. Qiu, J.-H. Chung, D. G. Nocera, and Y. S. Lee, Phys. Rev. Lett. **98**, 107204 (2007).

[3] Y. Okamoto, M. Nohara, H. Aruga-Katori, and H. Takagi, Phys. Rev. Lett. **99**, 137207 (2007).

[4] Y. Ran, M. Hermele, P. A. Lee, and X.-G. Wen, Phys. Rev. Lett. **98**, 117205 (2007).

[5] S. Yan, D. A. Huse, and S. R. White, Science **332**, 1173 (2011).

[6] S. Depenbrock, I. P. McCulloch, and U. Schollwöck, Phys. Rev. Lett. **109**, 067201 (2012).

[7] Y. Iqbal, F. Becca, S. Sorella, and D. Poilblanc, Phys. Rev. B **87**, 060405 (2013).

[8] H.-C. Jiang, Z. Wang, and L. Balents, Nat Phys **8**, 902 (2012).

[9] B. K. Clark, J. M. Kinder, E. Neuscamman, G. K.-L. Chan, and M. J. Lawler, Phys. Rev. Lett. **111**, 187205 (2013).

[10] T. Tay and O. I. Motrunich, Phys. Rev. B **84**, 020404 (2011).

[11] Y.-C. He, M. P. Zaletel, M. Oshikawa, and F. Pollmann, ArXiv e-prints (2016), arXiv:1611.06238 [cond-mat.str-el].

[12] H. J. Liao, Z. Y. Xie, J. Chen, Z. Y. Liu, H. D. Xie, R. Z. Huang, B. Normand, and T. Xiang, ArXiv e-prints (2016), arXiv:1610.04727 [cond-mat.str-el].

[13] H. J. Changlani and A. M. Läuchli, Phys. Rev. B **91**, 100407 (2015).

[14] B. S. Shastry and B. Sutherland, Physica B+C **108**, 1069 (1981).

[15] D. Yamamoto, G. Marmorini, and I. Danshita, Phys. Rev. Lett. **112**, 127203 (2014).

[16] D. Sellmann, X.-F. Zhang, and S. Eggert, Phys. Rev. B **91**, 081104 (2015).

[17] A. L. Chernyshev and M. E. Zhitomirsky, Phys. Rev. Lett. **113**, 237202 (2014).

[18] O. Götze and J. Richter, Phys. Rev. B **91**, 104402 (2015).

[19] K. Kumar, K. Sun, and E. Fradkin, Phys. Rev. B **90**, 174409 (2014).

[20] K. Kumar, H. J. Changlani, B. K. Clark, and E. Fradkin, Phys. Rev. B **94**, 134410 (2016).

[21] K. Essafi, O. Benton, and L. D. C. Jaubert, Nat Commun **7 SP -** (2016), article.

[22] C. D. Batista, Phys. Rev. B **80**, 180406 (2009).

[23] C. K. Majumdar and D. K. Ghosh, Journal of Mathematical Physics **10** (1969).

[24] D. J. Klein, Journal of Physics A: Mathematical and General **15**, 661 (1982).

[25] I. Affleck, T. Kennedy, E. H. Lieb, and H. Tasaki, Phys. Rev. Lett. **59**, 799 (1987).

[26] X.-G. Wen, Phys. Rev. Lett. **90**, 016803 (2003).

[27] A. Kitaev, Ann. Phys. **303**, 2 (2003).

[28] H. Wang, H. J. Changlani, Y. Wan, and O. Tchernyshyov, ArXiv e-prints (2017), arXiv:1702.01359 [cond-mat.str-el].

[29] A. B. Harris, C. Kallin, and A. J. Berlinsky, Phys. Rev. B **45**, 2899 (1992).

[30] C. L. Henley, Phys. Rev. B **80**, 180401 (2009).

[31] D. A. Huse and A. D. Rutenberg, Phys. Rev. B **45**, 7536 (1992).

[32] J. T. Chalker, P. C. W. Holdsworth, and E. F. Shender, Phys. Rev. Lett. **68**, 855 (1992).

[33] S. Sachdev, Phys. Rev. B **45**, 12377 (1992).

[34] O. Cépas and A. Ralko, Phys. Rev. B **84**, 020413 (2011).

[35] C. Castelnovo, C. Chamon, C. Mudry, and P. Pujol, Phys. Rev. B **72**, 104405 (2005).

[36] R. J. Baxter, Journal of Mathematical Physics **11**, 784 (1970).

[37] D. L. Bergman, C. Wu, and L. Balents, Phys. Rev. B **78**, 125104 (2008).

[38] F. Kolley, S. Depenbrock, I. P. McCulloch, U. Schollwöck, and V. Alba, Physical Review B **91**, 104418 (2015).

[39] S. Jiang, P. Kim, J. H. Han, and Y. Ran, arXiv preprint arXiv:1610.02024 (2016).

[40] I. Rousochatzakis, A. M. Läuchli, and F. Mila, Phys. Rev. B **77**, 094420 (2008).

[41] M. J. Lawler, H.-Y. Kee, Y. B. Kim, and A. Vishwanath, Phys. Rev. Lett. **100**, 227201 (2008).

[42] J. Kondev and C. L. Henley, Nuclear Physics B **464**, 540 (1996).

[43] V. Khemani, R. Moessner, S. A. Parameswaran, and S. L. Sondhi, Phys. Rev. B **86**, 054411 (2012).

[44] Y. Wan and M. J. P. Gingras, Phys. Rev. B **94**, 174417 (2016).

[45] Y.-H. Chan and L.-M. Duan, New Journal of Physics **14**, 113039 (2012).

[46] B. Normand and Z. Nussinov, Phys. Rev. Lett. **112**, 207202 (2014).

[47] M. Hermele, M. P. A. Fisher, and L. Balents, Phys. Rev. B **69**, 064404 (2004).

[48] D. A. Huse and V. Elser, Phys. Rev. Lett. **60**, 2531 (1988).

[49] H. J. Changlani, J. M. Kinder, C. J. Umrigar, and G. K.-L. Chan, Phys. Rev. B **80**, 245116 (2009).

[50] E. Neuscamman, H. Changlani, J. Kinder, and G. K.-L. Chan, Phys. Rev. B **84**, 205132 (2011).

FIGURE LEGENDS

Figure 1) **Three Coloring Point**

Figure 2) **Three Colorable lattices**

Figure 3) **Kagome phase diagram**

Figure 4) **Structure factor and fidelity**

Table 1) **Counting of three coloring solutions**

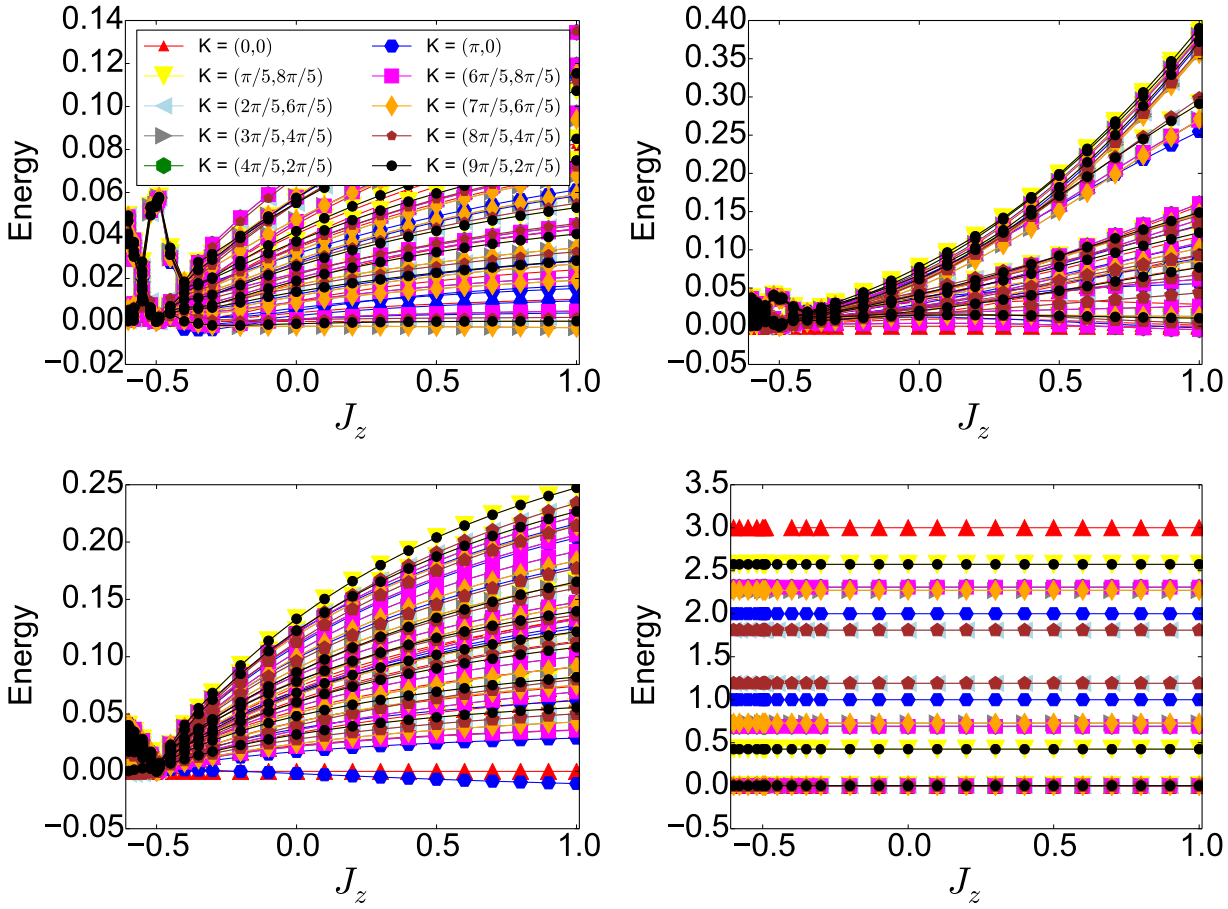

Figure 1. (Color online): The panels show energy gaps versus J_z (with respect to the lowest energy state in $K = (0, 0)$) for the 30 site kagome cluster with periodic boundary conditions. The panels correspond to various S_z sectors, (top left) $S_z = 0$, (top right) $S_z = 5$, (bottom right) $S_z = 10$, (bottom right) $S_z = 14$ (one-spin up). A quantum degeneracy is seen at $J_z = -1/2$. The case of $S_z = 14$ corresponds to the non-interacting solution, hence the spectrum is invariant to J_z.

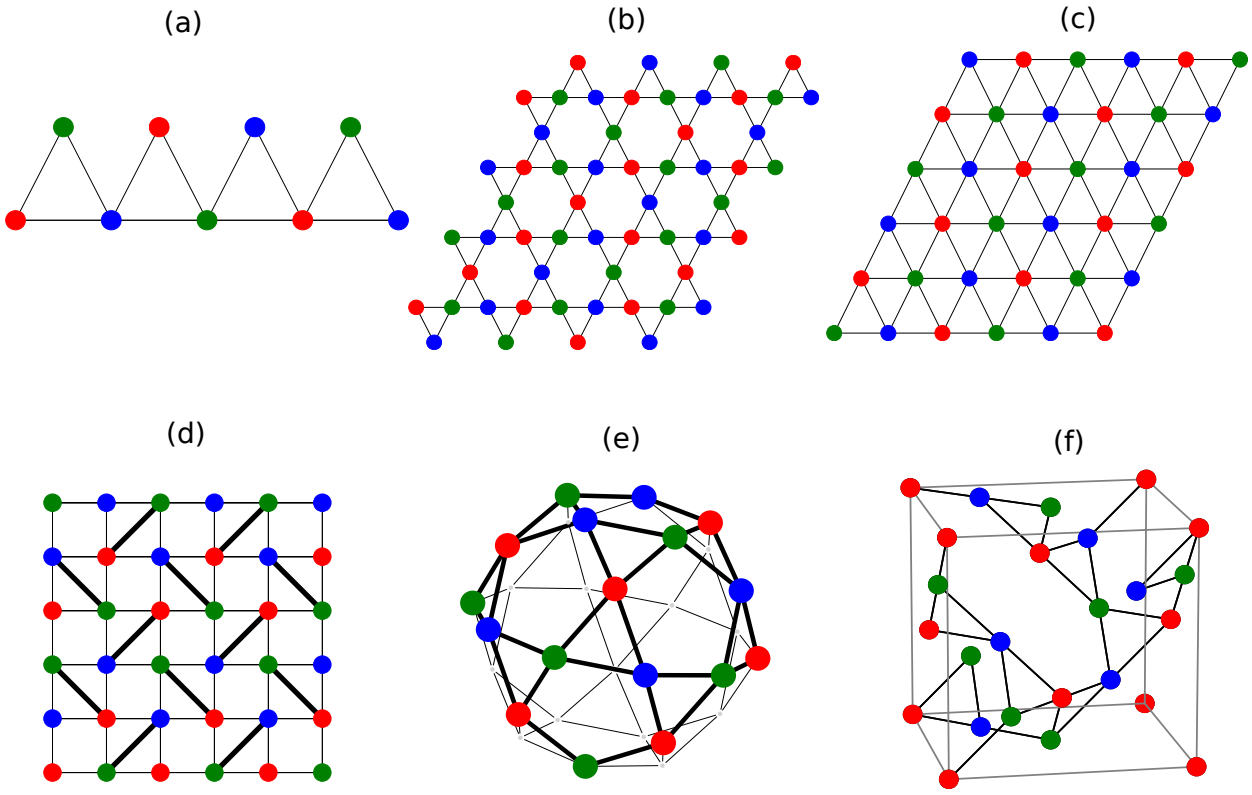

Figure 2. (Color online): Representative three coloring solutions on various lattices with triangular motifs in one, two, and three dimensions. (a) saw-tooth lattice (b) Kagome lattice (c) Triangular lattice (d) Shastry-Sutherland lattice (note here, the diagonal lines have two triangles overlapping it whereas every other edge has one overlapping triangle giving $J_2 = 2J_1$) (e) Icosidodecahedron (f) Hyperkagome lattice

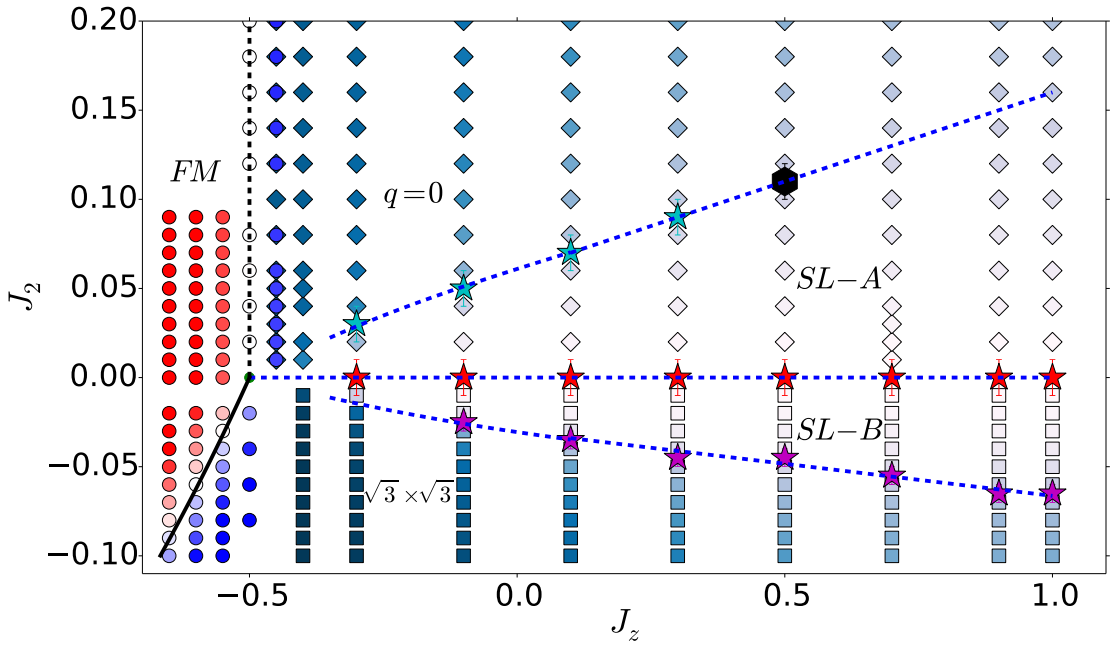

Figure 3. (Color online): The phase diagram in the $J_z - J_2$ plane on the 36d lattice. Circles correspond to the energy difference $E(S_z = 0)_{N=36} - E_{TDL}(S_z = N/2)$ between the $S_z = 0$ sector and fully polarized state ranging from deep blue (negative) to deep red (positive). The diamonds are colored based on the structure factor at the M point ($S(M)$) and squares are colored based on the structure factor at the K point ($S(K)$). The darkest color corresponds to the largest structure factor on the graph. Dotted lines are a guide to the eye. The solid line is where the energy difference between a fully polarized state and a un-projected $\sqrt{3} \times \sqrt{3}$ state goes to zero. Stars are fidelity dips. The diamond is a fidelity kink in the second derivative.

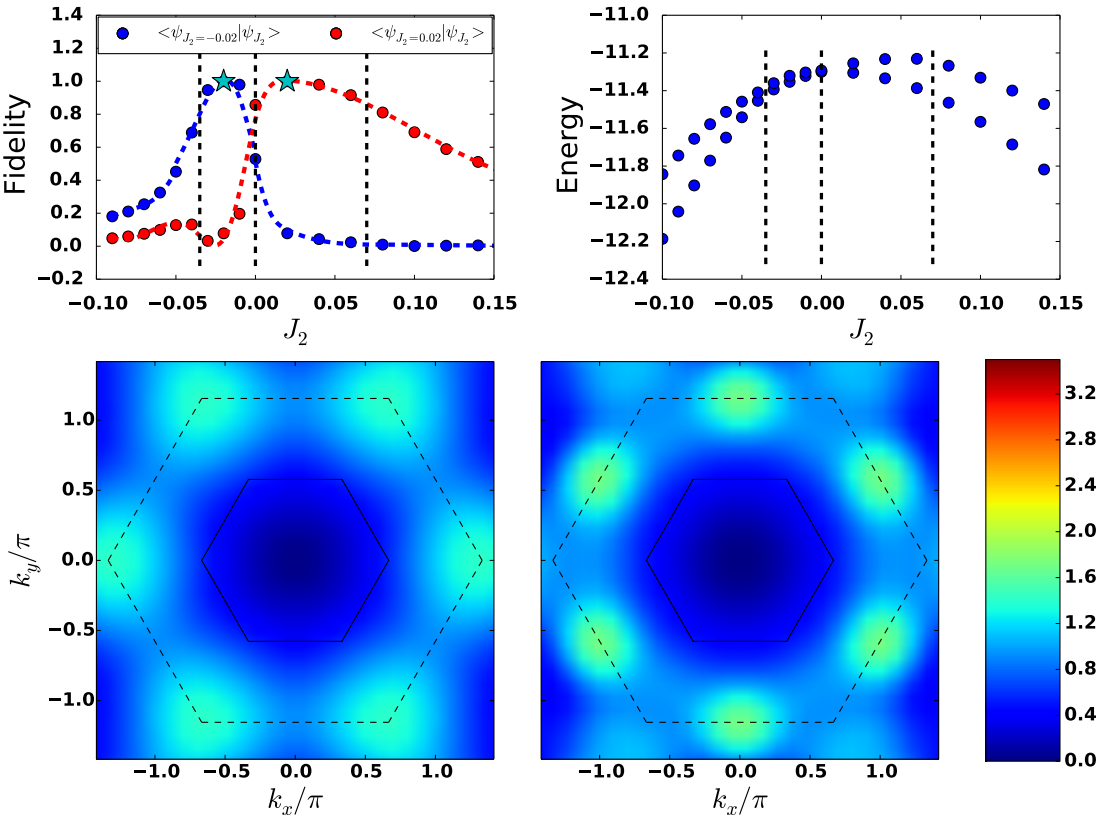

Figure 4. (Color online) All data is at $J_z = 0.1$. Top Left: Overlap of the ground state as a function of J_2 with $J_2 = -0.02$ (blue) and $J_2 = 0.02$ (red). Dashed lines represent transitions as measured by fidelity. Top Right: Energy of the two lowest states in the symmetric representation of $K = (0, 0)$ sector. There are additional state(s) between these two states in other quantum-number sectors. Bottom: Structure factors at $J_2 = -0.02$ (left) and $J_2 = 0.02$ (right)

Lattice	Method	$n_b = 1$	$n_b = 2$	$n_b = 3$	$n_b = 4$	$n_b = 5$	$n_b = 6$	# 3-colorings
sawtooth	ED	6	16	26	31	32	32	32
open $L = 5$	$R(S)$	6	16	26	31	32	32	
Husimi cactus	ED	5	11	15	16	16	15	16
$g = 1$	$R(S)$	5	11	15	16	16	15	
3×3 kagome obc	ED	15	102	414	1117			3808
(33 sites)	$R(S)$	15	102	414	1117	2136	3078	
3×3 kagome pbc	ED	10	38	60	41	40	40	40
	$R(S)$	10	34	40	40	40	40	
5×2 kagome pbc	ED	11	47	92	83	65	64	64
	$R(S)$	11	42	58	63	64	64	
4×3 kagome pbc	ED	13	68	169	172	137	136	136
	$R(S)$	13	68	134	136	136	136	

Table I. Number of ground states for different hard-core boson number (n_b) on several lattices with triangular motifs at $J_z = -1/2$, $J_2 = 0$. $R(S)$ is the rank of the overlap matrix indicating the number of linearly independent 3-coloring modes while ED refers to the exact number of ground states seen in a full diagonalization or Lanczos calculation. The kagome cluster with open boundary conditions has completed triangles, resembling the periodic counterpart in appearance. For all the clusters with open boundaries, there were no additional non-3 coloring ground states for all fillings. For the kagome clusters on tori, additional ground states are found especially at some low fillings.